Journal of Control, Automation and Electrical Systems (2023) 34:1080–1092
https://doi.org/10.1007/s40313-023-01030-4

Multi-objective Optimization Approach for Allocation and Sizing of Distributed Energy Resources Preserving the Protection Scheme in Distribution Networks

Renato S. F. Ferraz[1] · Rafael S. F. Ferraz[1] · Augusto C. Rueda–Medina[1]

Received: 7 October 2022 / Revised: 12 June 2023 / Accepted: 31 July 2023 / Published online: 14 August 2023

Abstract
In this paper, a multi-objective optimization approach to solve the problem of optimal allocation and sizing of inverter-based distributed energy resources (DERs) in distribution systems is presented. The objectives of this allocation and sizing problem consist of the minimization of the investment and operation costs, the voltage deviation and the short-circuit currents. The recloser–fuse coordination constraints were included in the mathematical formulation of the problem, in order to preserve the original network protection scheme. It is important to mention that this protection scheme was also carried out in this paper, using the multi-objective approach, to minimize the operating time of the reclosers and fuses. The distribution system considered to evaluate the proposed methodology was the IEEE 34-Node Test Feeder, and the non-dominated sorting genetic algorithm II was used to solve the proposed multi-objective problems. Furthermore, a time-series-based probabilistic approach, through the Monte Carlo simulation, was adopted to deal with the uncertainties of the load and power generated by each DER. Finally, from the results, it was possible to reduce the investment and operation costs by 15.61% when compared to the system without DERs, improve the voltage profile and preserve the original protection scheme present in the network.

Keywords Distributed energy resource · Non-dominated sorting genetic algorithm II · Protection system · Short-circuit currents

1 Introduction

Currently, it is possible to notice the high integration of inverter-based distributed energy resources (DERs) in distribution systems, which promotes several benefits in the network. Nevertheless, depending on the DER location and size, the power system protection may not operate as desired, due to the modified load and short-circuit currents of the system (Blaabjerg et al., 2017). For this reason, some studies have been carried out to evaluate the impacts caused by the DER integration in the protection schemes (Blaabjerg et al., 2017; Usama et al., 2021; Meskin et al., 2020). From the review performed in these papers, it is possible to notice that many methodologies have been proposed to mitigate the problems of the DERs on the power systems, with emphasis on the adaptive protection schemes, the application of fault current limiter (FCL), and the adjustment of the protective device settings considering the DER integration in the distribution system.

Adaptive protection consists of the modification of protective settings to address changes in the network through external control signals. Shah and Bhalja (2014) and Alam (2019) proposed adaptive protection schemes for power distribution networks containing DERs, through the modification of the relays settings. An adaptive protection, based on the differential evolution algorithm, was adopted by Shih et al. (2017) to reduce the DER impacts on the protective devices and improve the overall sensitivity of directional overcurrent relay. Jain et al. (2019) and Purwar et al. (2020) proposed an adaptive protection to guarantee the correct operation of the protective devices for different operating conditions of the system, including loss of loads, generators

✉ Renato S. F. Ferraz
renato.s.ferraz@edu.ufes.br

Rafael S. F. Ferraz
rafael.ferraz@edu.ufes.br

Augusto C. Rueda–Medina
augusto.rueda@ufes.br

[1] Postgraduate Program in Electrical Engineering, Federal University of Espírito Santo, Av. Fernando Ferrari, Vitória, Espírito Santo 29075-910, Brazil

and lines. The drawback of the online adaptive protection is the need for reliable and fast communication channels to update the relay or recloser settings, whereas the offline methods require complex calculations to consider all the system conditions and can fail if unexpected circumstances occur.

The FCL is a superconductor device which limits the magnitude of current during a fault. Elmitwally et al. (2016) used the particle swarm optimization to restore the coordination between the protective devices in distribution systems with high DER integration, through the allocation of FCL. Optimization algorithms were adopted by Shu et al. (2021) and Dahej et al. (2018), in order to allocate FCL devices, aiming to reduce costs and mitigate the effects of the fault current. Hamidi and Chabanloo (2019) and El-Ela et al. (2021) performed the optimal allocation of different types of DERs correlated with FCL devices using, respectively, non-dominated sorting genetic algorithm II (NSGA-II) and Coyote optimization algorithm. In addition, Cuckoo optimization algorithm and linear programming were combined by Dehghanpour et al. (2018) to optimize the coordination of protective devices and find the optimized value of FCL at the point of common coupling. However, the use of FCL devices, in the distribution system with high DER penetration levels, increases the operating time of the protective devices when the DER is out of service. Furthermore, the prohibitive cost of FCL may limit the wide installation of this device in the networks.

On the other hand, some methodologies, based on the adjustment of the protective device settings, have been proposed to mitigate the issues caused by the DER integration. Ferraz et al. (2020) used the genetic algorithms method to achieve the optimized recloser–fuse coordination taking into account the DER operating modes and all the fault types. Fani et al. (2018) changed the characteristic curve of the relay in order to ensure the coordination of these devices considering different DER penetration levels and locations. A multi-objective approach, based on NSGA-II, was adopted by Pereira et al. (2018) to obtain the optimized coordination of protective devices, through the minimization of the investment and interruption costs. Alam et al. (2018) and Sharma and Panigrahi (2018) introduced single protection schemes, considering the network with multiple dispersed generators. Despite the benefits of resizing the protective devices, this method degrades the sensitivity of the protection scheme, mainly, when the DER is not operating, in addition to increasing the investment costs, through the replacement of reclosers, relays and fuses.

Recently, multi-objective optimization approaches have been adopted to allocate and size DERs in distribution systems. Huang et al. (2019) used the multi-objective estimation of distribution algorithm with the purpose of allocating and sizing DERs to reduce the overall costs of the system. Priya et al. (2022) proposed a new long-term planning methodology for multi-objective DER placement and sizing aiming to minimize the power losses, carbon dioxide emission, overall cost, besides enhancing the system voltage stability and reliability. A new multi-objective optimization model was presented by Ahmadi et al. (2021) to improve the voltage profile and minimize DERs and battery costs through the allocation and sizing DERs and battery systems. Abdelaziz and Moradzadeh (2019) used the NSGA-II to solve the multi-objective DERs allocation problem considering the Monte Carlo simulation (MCS). A fuzzy embedded multi-objective particle swarm optimization technique was used by Roy and Das (2021) to allocate DERs considering renewable generation and load demand uncertainties. Nevertheless, none of these papers, regarding the optimized positioning of DERs, considered the negative impacts of the DERs integration on the protection system.

Table 1 shows the main contributions of this paper against the previously mentioned works. It evaluated the optimization approach, whether multi-objective or single-objective; the DERs allocation; the recloser–fuse coordination; the inclusion of uncertainties in the problem formulation; and the 24-hour analysis.

Based on Table 1, it is possible to notice that most of the papers did not consider the uncertainties of the load and power generated by the DERs. The stochastic characteristic of these variables interferes directly in the adjustment of protective devices. In addition, the load and DER generation variation during the day were not regarded in the majority of studies, which modifies the load and short-circuit current in the distribution feeder. Besides that, some studies only take the reclosers coordination into account, disregarding the coordination of the reclosers, in fast and slow mode, with the fuses; however, it is essential to implement fuses in the problem formulation, to achieve greater protection selectivity and cost reduction.

Therefore, in this paper, a multi-objective optimization approach was adopted for the allocation and sizing of inverter-based DERs, to minimize the investment and operation costs, voltage deviation and short-circuit current. In addition to the operational constraints of the distribution system, this optimization problem included the recloser–fuse coordination constraints, in order to preserve the original protection scheme of the network, avoiding the need for adaptive protection schemes, application of FCL or modification of the protective device settings. Furthermore, the distribution system used to evaluate the proposed methodology was the IEEE 34-Node Test Feeder (Kersting, 2001), and the NSGA-II was adopted to solve the multi-objective problem formulated in this study (Deb et al., 2002). The main contributions of this paper are as follows:

1. The recloser–fuse coordination scheme was carried out using the NSGA-II algorithm to minimize the operating

Table 1 Proposed approach compared to other papers

Paper	Opt. approach	DERs allocation	Recloser–fuse coord.	Uncert.	24-Hour analysis
Shah and Bhalja (2014)	×	×	✓	×	×
Alam (2019)	SO	×	×	×	×
Shih et al. (2017)	SO	×	×	×	✓
Jain et al. (2019)	×	×	×	×	✓
Purwar et al. (2020)	SO	×	×	×	×
Elmitwally et al. (2016)	SO	×	✓	×	×
Shu et al. (2021)	MO	×	×	✓	×
Dahej et al. (2018)	SO	×	×	×	×
Hamidi and Chabanloo (2019)	MO	✓	×	×	✓
El-Ela et al. (2021)	MO	✓	×	×	×
Dehghanpour et al. (2018)	SO	×	×	×	×
Ferraz et al. (2020)	SO	✓	✓	×	✓
Fani et al. (2018)	×	×	✓	×	×
Pereira et al. (2018)	MO	×	✓	×	×
Alam et al. (2018)	SO	×	✓	×	×
Sharma and Panigrahi (2018)	SO	×	×	×	×
Huang et al. (2019)	MO	✓	×	✓	×
Priya et al. (2022)	MO	✓	×	✓	✓
Ahmadi et al. (2021)	MO	✓	×	×	✓
Abdelaziz and Moradzadeh (2019)	MO	✓	×	✓	✓
Roy and Das (2021)	MO	✓	×	✓	✓
Proposed paper	MO	✓	✓	✓	✓

✓: Yes, ×: No, *SO* single-objective, *MO* multi-objective

time of the reclosers, in the fast and slow mode, and the operating time of the fuses;
2. The mathematical formulations, proposed in this paper, considered a time-series-based probabilistic approach, through the MCS, in order to include the uncertainties of the loads and power generated by each DER;
3. For normal condition, the DER reactive power capability was based on the nonlinear operational limits established in the Standard IEEE 1547-2018, whereas for fault condition, voltage-dependent control strategies were adopted.

The remainder of the paper is organized as follows: In Sects. 2 and 3, the recloser–fuse coordination and DER allocation problems, respectively, are presented. In Sect. 4, the proposed algorithm is depicted. In Sect. 5, the tests and results regarding the optimization problems are shown. Finally, concluding remarks are provided in Sect. 6.

2 Recloser–Fuse Coordination Problem

The multi-objective programming approach used to solve the optimized coordination of the protective devices consists of minimizing the operating time of the reclosers, in the fast and slow mode, and the operating time of the fuses. The fuse saving scheme was adopted in this paper to avoid permanent outages during temporary faults, since the fuses require physical replacement after a fault clearing operation (Ferraz et al., 2020). This protection scheme reduces the cost to replace the fuses and the outage time.

Figure 1a presents an example of a distribution system protected by two reclosers and two fuses in series. It is important to mention that the mathematical formulation, provided in this section to perform the recloser–fuse coordination, is feasible for other system configurations. Figure 1b shows a flowchart with the sequence of recloser–fuse operation for providing selective protection, considering the fuse saving scheme. On the side of the flowchart, the minimum coordination time intervals between two protective devices are depicted. In Fig. 1, R_n is the recloser; F_k is the fuse; $T_{R_n,\mathrm{sm}}$ and $T_{R_n,\mathrm{fm}}$ are the operating time of the recloser in slow and fast mode, respectively; T_{F_k} is the operating time of the fuse; and CTI is the coordination time interval. Based on the operation sequence presented in Fig. 1, it is possible to incorporate the recloser–fuse coordination constraints into the problem formulation.

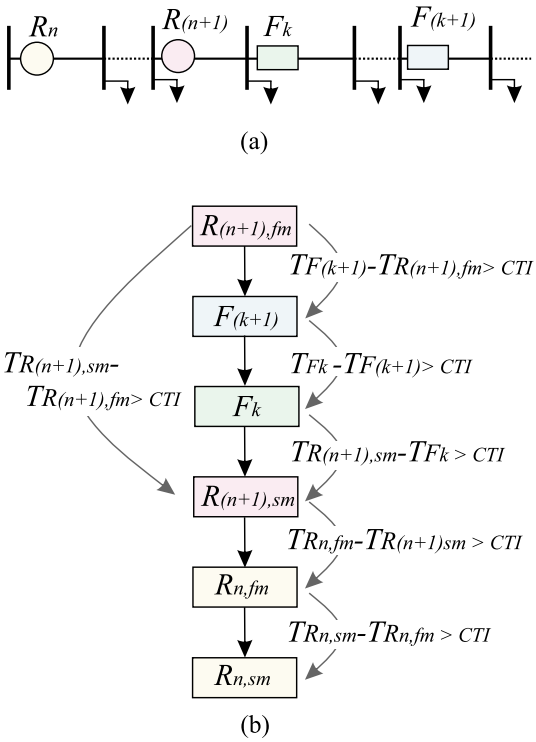

Fig. 1 **a** Distribution system example and **b** flowchart to demonstrate the protection scheme

The mathematical formulation for the recloser–fuse coordination problem is presented in Eqs. (1)–(12).

$$\min \; f_1 \sum_{h=1}^{h_m} \sum_{f=1}^{f_m} \sum_{z=1}^{z_m} \sum_{s=1}^{s_m} \sum_{n=1}^{n_m} T_{R_n,fm,h,f,z,s} \tag{1}$$

$$\min \; f_2 \sum_{h=1}^{h_m} \sum_{f=1}^{f_m} \sum_{z=1}^{z_m} \sum_{s=1}^{s_m} \sum_{n=1}^{n_m} T_{R_n,sm,h,f,z,s} \tag{2}$$

$$\min \; f_3 \sum_{h=1}^{h_m} \sum_{f=1}^{f_m} \sum_{z=1}^{z_m} \sum_{s=1}^{s_m} \sum_{k=1}^{k_m} T_{F_k,h,f,z,s} \tag{3}$$

subject to

$$\mathrm{TMS}_{n,\mathrm{sm}}^{\min} \le \mathrm{TMS}_{n,\mathrm{sm}} \le \mathrm{TMS}_{n,\mathrm{sm}}^{\max} \tag{4}$$

$$\mathrm{TMS}_{n,\mathrm{fm}}^{\min} \le \mathrm{TMS}_{n,\mathrm{fm}} \le \mathrm{TMS}_{n,\mathrm{fm}}^{\max} \tag{5}$$

$$Ip_n^{\min} \le Ip_n \le Ip_n^{\max} \tag{6}$$

$$T_{F_{(k+1)}} - T_{R_{(n+1),\mathrm{fm}}} > \mathrm{CTI} \tag{7}$$

$$T_{F_k} - T_{F_{(k+1)}} > \mathrm{CTI} \tag{8}$$

$$T_{R_{(n+1),\mathrm{sm}}} - T_{F_k} > \mathrm{CTI} \tag{9}$$

$$T_{R_{n,\mathrm{fm}}} - T_{R_{(n+1),\mathrm{sm}}} > \mathrm{CTI} \tag{10}$$

$$T_{R_{n,\mathrm{sm}}} - T_{R_{n,\mathrm{fm}}} > \mathrm{CTI} \tag{11}$$

$$T_{R_{(n+1),\mathrm{sm}}} - T_{R_{(n+1),\mathrm{fm}}} > \mathrm{CTI} \tag{12}$$

where the indices h, f, z, s, n, and k are, respectively, hours of the day, fault types, fault locations, scenarios generated by the MCS, reclosers, and fuses; the index m is the maximum value of each variable; Ip_n is the pick-up current of the recloser R_n; and $\mathrm{TMS}_{n,\mathrm{sm}}$ and $\mathrm{TMS}_{n,\mathrm{fm}}$ are the time multiplier setting of R_n in slow and fast mode, respectively.

The objective functions (1)–(3) are, respectively, the operating time of the reclosers in fast mode, the reclosers in slow mode and the fuses. Equations (4)–(6) represent the limits of the setting parameters of the reclosers; Eqs. (7) and (9) are the recloser–fuse coordination based on the fuse saving scheme; Eq. (8) corresponds to the coordination interval of the fuses; Eq. (10) is the coordination interval of the reclosers, whereas Eqs. (11) and (12) depict the coordination interval of the recloser in slow and fast mode.

Furthermore, the fuse characteristic curve is represented by a log-log function, depicted in Eq. (13), which depends on the fuse characteristic coefficients a_k and b_k (Alam et al., 2018; Ferraz et al., 2020), whereas the inverse time recloser has a characteristic curve, which can act in a fast or slow mode, described, respectively, in Eqs. (14) and (15) (IEC, 1989).

$$\log(T_{F_k}) = a_k \log(I) + b_k \tag{13}$$

$$T_{R_n,\mathrm{fm}} = \mathrm{TMS}_{n,\mathrm{fm}} \left[\frac{K}{\left(\frac{I}{Ip_n}\right)^{\alpha} - 1} \right] \tag{14}$$

$$T_{R_n,\mathrm{sm}} = TMS_{n,\mathrm{sm}} \left[\frac{K}{\left(\frac{I}{Ip_n}\right)^{\alpha} - 1} \right] \tag{15}$$

where I is the current flowing through each protective device; and K and α are constants according to the recloser type of curve.

3 Distributed Energy Resource Allocation Problem

The multi-objective programming approach, adopted to achieve the optimized size and location of DER, consists of minimizing the annualized investment and operation costs of the system, the voltage deviation and the short-circuit current. The mathematical formulation for the DER allocation problem is presented in Eqs. (16)–(29).

$$\min \; f_4 \sum_{s=1}^{s_m} \sum_{g=1}^{g_m} \sum_{t=1}^{t_m} z_{g,t} C_t + 365 \sum_{s=1}^{s_m} \sum_{h=1}^{h_m} \left(ec^S P_{h,s}^S + \sum_{g=1}^{g_m} ec^{DER} P_{h,g,s}^{DER} \right) \tag{16}$$

$$\min \; f_5 \sum_{h=1}^{h_m} \sum_{g=1}^{g_m} \sum_{s=1}^{s_m} |V_{h,g,s} - 1| \tag{17}$$

$$\min \; f_6 \sum_{h=1}^{h_m} \sum_{f=1}^{f_m} \sum_{z=1}^{z_m} \sum_{s=1}^{s_m} IF_{h,f,z,s} \tag{18}$$

subject to
constraints (7)–(12),

$$i_{h,j,s} \leq i_j^{\max} \tag{19}$$

$$V^{\min} \leq V_{h,g,s} \leq V^{\max} \tag{20}$$

$$\sum_{g=1}^{g_m} \sum_{t=1}^{t_m} z_{g,t} \leq n_{\text{DER}}^{\max} \tag{21}$$

$$\sum_{t=1}^{t_m} z_{g,t} \leq 1 \tag{22}$$

$$\frac{P_{h,s}^S}{S_{h,s}^S} \geq \left(\frac{P^S}{S^S}\right)^{\max} \tag{23}$$

$$\sum_{g=1}^{g_m} \left(P_{h,g}^{\text{load}} - Re\left\{V_{h,g} i_{h,g}^* - Y_g^* |V_{h,g}|\right\}\right) = 0 \tag{24}$$

$$\sum_{g=1}^{g_m} \left(Q_{h,g}^{\text{load}} - Im\left\{V_{h,g} i_{h,g}^* - Y_g^* |V_{h,g}|\right\}\right) = 0 \tag{25}$$

$$\left(P_{h,g,s}^{\text{DER}}\right)^2 + \left(Q_{h,g,s}^{\text{DER}}\right)^2 \leq (S_{\text{rated}})^2 \tag{26}$$

$$P_{h,g,s}^{\text{DER}} \geq 0.05 \; S_{\text{rated}} \tag{27}$$

$$-0.44 \; S_{\text{rated}} \leq Q_{h,g,s}^{\text{DER}} \leq 0.44 \; S_{\text{rated}} \tag{28}$$

$$-2.2 \; P_{h,g,s}^{\text{DER}} \leq Q_{h,g,s}^{\text{DER}} \leq 2.2 \; P_{h,g,s}^{\text{DER}} \tag{29}$$

where the indices j, g and t are, respectively, branches, nodes and DER types; $z_{g,t}$ is a binary variable for the allocation of DER of type t at node g; C_t is the annualized installation cost of the DER of type t (in US$); ec^{DER} and ec^S are, respectively, the energy cost for the DER and substation (in US$/kWh); $P_{h,g,s}^{\text{DER}}$ and $P_{h,s}^S$ are, respectively, the active power provided by the DER and substation; $V_{h,g,s}$ is the nodal voltage; and $IF_{h,f,z,s}$ is the short-circuit current. In addition, $i_{h,j,s}$ is the current in the branch j; $n_{\text{DER}}^{\max}$ is the number of DER available for allocation; $Q_{h,g,s}^{\text{DER}}$ is the reactive power provided by the DER; S_{rated} is the rated apparent power of the inverter-based DER; $S_{h,s}^S$ is the apparent power provided by the substation; $P_{h,g,s}^{\text{load}}$ and $Q_{h,g,s}^{\text{load}}$ are, respectively, the load active and reactive power values at node g; $i_{h,g,s}$ is the current injection at node g; and Y_g is the shunt admittance at node g. Furthermore, Re and Im, in Eqs. (24) and (25), are respectively, the real and imaginary parts of the complex values.

The objective function presented in Eq. (16), consists of the minimization of the overall system cost. The first term of this equation is the annualized investment cost of the DER, the second one is the substation annual operation cost, and the third one is the DER annual operation cost. On the other hand, the objective function shown in Eq. (17) aims to minimize the voltage deviation of the network nodes, in order to improve the voltage profile. The objective function depicted in Eq. (18) consists of the minimization of the short-circuit currents of the system. It is important to mention that the objective function (18) was included in this formulation to reduce the negative impacts caused by the DER integration. Equations (7)–(12) are the constraints which guarantee the proper coordination of the protective devices even with the DER integration. Equations (19) and (20) are the system operational constraints regarding the voltage and current, respectively. The maximum number of DER available for allocation is represented by Eq. (21), whereas Eq. (22) ensures that only one DER can be allocated in each node of the system. Equation (23) specifies the limit of the leading or lagging substation power factor. The active and reactive power balance in the distribution system are represented, respectively, in Eqs. (24) and (25).

In this paper, the DER reactive power capability was based on the Standard IEEE 1547-2018, which specifies the attributes of reactive and active power control requirements of the inverters (IEEE, 2018). According to this standard, the inverters, associated with each DER, can operate in Category A or B. In this regard, DER with Category B performance covers all requirements within Category A and specifies supplemental capabilities needed to correctly integrate DERs in the systems, where the DER penetration level is high (IEEE, 2018). Therefore, in this work, the inverters associated with each DER must operate in Category B, to deal with power quality issues caused by the high penetration level of DER. Equations (26)–(29) depict the constraints regarding the reactive power capability for Category B, which is shown in Fig. 2.

4 Proposed Algorithm

The problem discussed in this paper consists of the optimized allocation of inverter-based DER in a distribution system, considering the recloser–fuse coordination constraints in the mathematical formulation in order to preserve the original protection scheme. The flowchart, which summarizes the proposed algorithm, is shown in Fig. 3.

In Block A, the initial population, which represents the DER location and size, is randomly generated. The codification of each individual is represented by δ binary variables, which indicate the presence of DER in each network node, and by the active and reactive power generated by each DER, where δ is the number of nodes of the system.

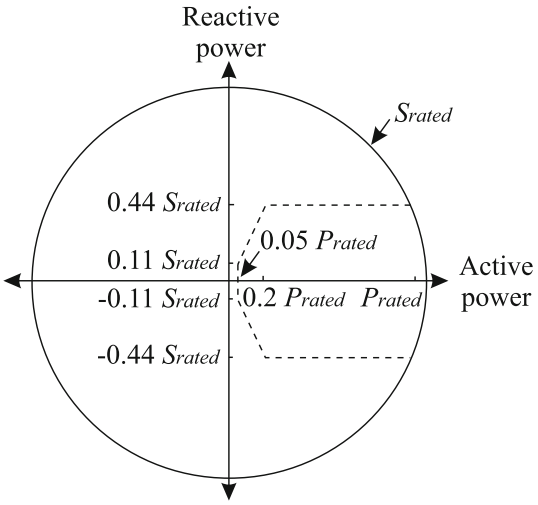

Fig. 2 Reactive power capability for DERs in category B defined in IEEE 1547-2018

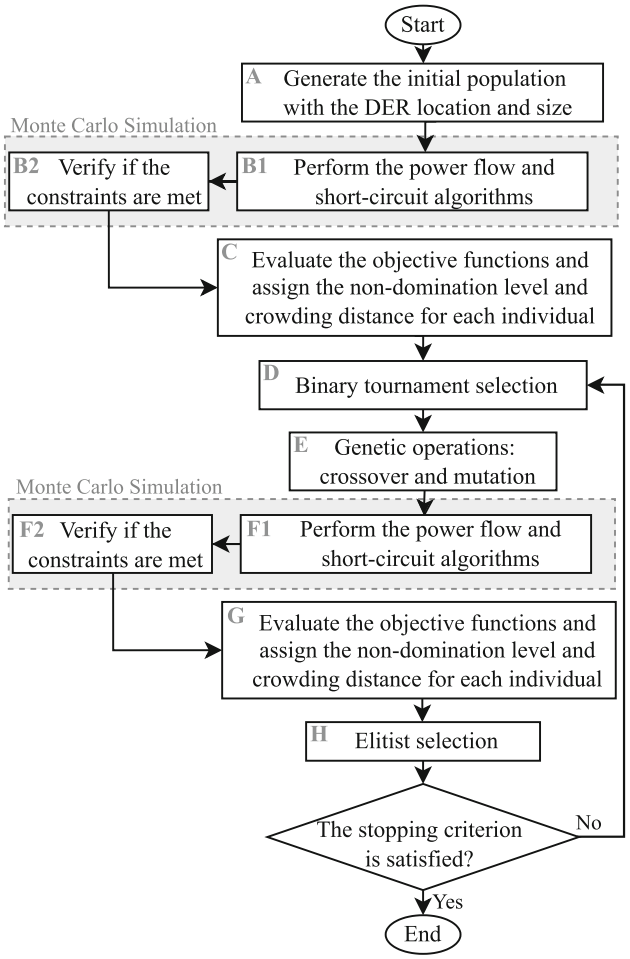

Fig. 3 Flowchart of the proposed algorithm

From the individuals of this population, it is necessary to compute the power flow and achieve the short-circuit currents (Block B1). In this study, the short-circuit current considered the contribution of the load currents, since it may affect the operation of the protective devices (Mathur et al., 2015). Furthermore, the fault current contribution of the inverter-based DER was computed based on the methodology proposed by Mathur et al. (2017), which takes into account different voltage-dependent control modes, to improve the voltage profile of the system during fault conditions. The three-phase power flow solution method used was the backward–forward sweep, due to its simplicity, low computational effort and high accuracy (Cheng & Shirmohammadi, 1995). This iterative algorithm can be summarized in three steps: (a) the nodal current calculation; (b) the backward sweep to sum up the line section current; and (c) the forward sweep to update nodal voltage. A more in-depth discussion of this method and its applications is presented by Cheng and Shirmohammadi (1995).

The MCS consists of repeated random sampling to obtain numerical results, based on the law of large numbers and the central limit theorem. From this sampling, it is possible to estimate the behavior of a system or a process that involves stochastic variables. For this reason, the MCS was adopted in Blocks B1 and B2, to deal with the uncertainties of the loads and power generated by each DER. Therefore, the power flow and the fault analysis must be performed for all the probabilistic scenarios generated by the MCS to verify if the constraints are met.

The objective functions, presented in Eqs. (16)–(18), are evaluated in Block C, in order to compute the non-domination levels and the crowding distance of each individual. In Blocks D and E, the genetic operators (binary tournament selection, crossover and mutation) are performed, and the offspring population is evaluated. For this evaluation, the power flow and the fault analysis are performed for all the probabilistic scenarios generated by the MCS (Blocks F1, F2 and G). Finally, the best individuals are chosen in Block H through an elitist selection, and it is verified if the stopping criterion is satisfied. The solutions generated by this algorithm consist of the optimized size and location of the DERs, which reduces the investment and operation costs, voltage deviation and short-circuit current, while preserving the protection scheme of the network.

5 Results and Discussion

In this section, the results regarding the coordination of protective devices and the allocation of DERs will be described

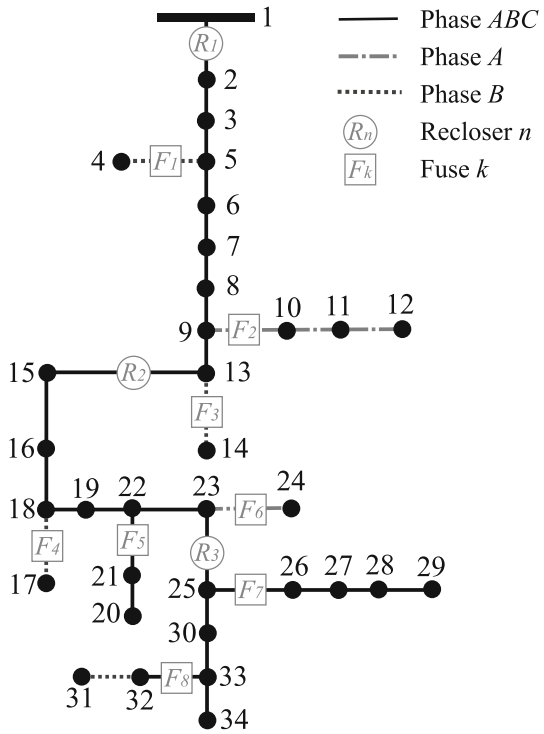

Fig. 4 Representation of the IEEE 34-Node Test Feeder with the reclosers and fuses

in detail. The IEEE 34-Node Test Feeder, shown in Fig. 4, was adopted to evaluate the proposed methodology. The voltage regulators in this test system were disregarded in order to verify if the DERs can improve the voltage profile. The protection scheme, presented in Fig. 4, consists of three reclosers in the primary branch and eight fuses in the branches that are derived from the primary branch. Considering the fuse saving scheme, the reclosers must protect the system from temporary faults, whereas the fuses must provide primary protection against permanent faults.

The proposed algorithm has been implemented using the C++ programming language with a workstation PC with an AMD Ryzen 7 4800H processor and 16 GB DDR4 3200 MHz of RAM. The NSGA-II simulation was performed considering a population of 60 individuals, with a crossover probability of 90%, a mutation probability of 10% and a maximum number of generations of 400. The computing time for the optimized coordination of protective devices, presented in Sect. 5.1, was 3.357 s, whereas the computing time for the optimized DER allocation, presented in Sect. 5.2 was 235.548 s. Initially, the load and short-circuit currents of the IEEE 34-Node Test Feeder were achieved in Subsection 5.1. Thereafter, the NSGA-II was adopted to coordinate reclosers and fuses present in the network, aiming to minimize the operating time of these devices. In Sect. 5.2, the NSGA-II was adopted to allocate and size DERs preserving the protection scheme of the system.

5.1 Coordination of the Protective Devices

Initially, the coordination of the protective devices was performed without taking the system DERs into account. In this paper, only reclosers with very inverse curves were considered, according to the International Electrotechnical Commission (IEC, 1989). Moreover, $Ip_n^{\max}$ was adjusted based on the smallest short-circuit current passing through the analyzed recloser multiplied by 2/3 (Ferraz et al., 2020), whereas $Ip_n^{\min}$ was set in accordance with the highest load current at the branch where the recloser R_n was inserted, multiplied by an overload factor of 25% (Alam et al., 2018). The maximum and minimum time multiplier setting values adopted were 0.05 and 1 s, respectively (Dehghanpour et al., 2018). It was assumed that the constant a is equal for the eight fuses, in order to reach the same type of fuse for all the system. The CTI value, assumed in this paper, was 0.2 s (Sharma & Panigrahi, 2018).

Table 2 shows the minimum and maximum short-circuit currents passing through the protective devices considering 3-line-to-ground (3LG), line-to-line (2L), 2-line-to-ground (2LG) and line-to-ground (LG) faults. The minimum and maximum short-circuit current values, for all fault types, are highlighted in bold for each protection device. Additionally, Table 2 presents the minimum and maximum load currents passing through the protective devices. These values were considered to set $Ip_n^{\min}$ and $Ip_n^{\max}$.

Tables 3 and 4 present the optimized parameters of the protective devices that were achieved considering the mathematical formulation of the recloser–fuse coordination problem.

Based on the determination of the characteristic coefficients a_k and b_k for each fuse, it becomes feasible to define commercially available fuses that effectively integrate the proposed protection scheme presented in this paper. For fuses F_1–F_8, the Bussmann series 5.5 kV E-Rated medium voltage fuses for feeder circuits, specifically the MV055 model, were adopted with the following current ratings: 50 A, 30 A, 40 A, 25 A, 20 A, 20 A, 20 A, and 20 A, respectively (Eaton, 2018).

Then, using the optimized parameters in Eqs. (14) and (15), in addition to the characteristic curve of the fuses previously mentioned, it is possible to reach the coordination between each fuse and its nearest upstream recloser, depicted in Fig. 5. The minimum and maximum short-circuit current values for each fuse, presented in Table 2, are highlighted in red in the graphs of Fig. 5. Furthermore, the difference in operation time of the protective devices for the aforementioned short-circuit current values was also presented in Fig. 5, aiming to demonstrate that the constraints (7)–(12) were met, since the coordination interval is higher than CTI.

From Fig. 5, it is possible to notice that the reclosers in fast mode will operate for temporary faults, in order to preserve

Table 2 Fault and load minimum and maximum currents measured at the reclosers and fuses

	3LG fault [A]		2L fault [A]		2LG fault [A]		LG fault [A]		Load [A]	
	Min	Max	Min	Max	Min	Max	Min	Max	Min	Max
R_1	118.41	644.67	**94.47**	554.84	112.71	652.24	105.55	**665.38**	13.22	45.42
R_2	117.48	**293.62**	**93.49**	263.71	110.81	280.77	102.50	252.10	9.40	31.92
R_3	195.41	**201.85**	163.36	181.32	178.21	187.94	**158.43**	173.95	5.76	19.81
F_1	–	–	–	–	–	–	**416.40**	**417.21**	0.14	0.58
F_2	–	–	–	–	–	–	**160.76**	**266.67**	3.25	12.65
F_3	–	–	–	–	–	–	**242.39**	**246.21**	0.37	1.47
F_4	–	–	–	–	–	–	**180.59**	**182.45**	0.03	0.14
F_5	113.77	**120.44**	**97.24**	106.03	108.21	115.33	100.75	108.01	2.42	11.25
F_6	–	–	–	–	–	–	**166.71**	**170.76**	0.02	0.07
F_7	195.17	**201.58**	164.57	181.29	178.14	187.66	**158.64**	170.14	3.81	14.41
F_8	195.92	**197.12**	170.59	178.85	178.84	182.84	**158.27**	165.89	0.51	1.97

3LG 3-line-to-ground, *2L* line-to-line, *2LG* 2-line-to-ground, *LG* line-to-ground

Table 3 Solution of the NSGA-II regarding the recloser parameters

	Recloser		
	R_1	R_2	R_3
TMS_{sm} $[s]$	0.90	0.45	0.80
TMS_{fm} $[s]$	0.20	0.10	0.05
Ip $[A]$	60.00	54.00	25.00

Table 4 Solution of the NSGA-II regarding the fuse parameters

Fuse	a	b		a	b
F_1	−1.26	7.26	F_5	−1.26	6.44
F_2	−1.26	7.01	F_6	−1.26	6.32
F_3	−1.26	6.99	F_7	−1.26	5.51
F_4	−1.26	6.46	F_8	−1.26	5.49

the fuse saving scheme. The fuses will actuate for permanent faults and, for backup protection, the recloser in slow mode shall operate. For this reason, the fuses curves lie well inside the operating times of the reclosers, as shown in Fig. 5. Nevertheless, for the faults which occur in the primary branch, where there are no upstream fuses, the reclosers will protect the feeder from permanent and temporary faults. Therefore, based on the coordination curves, presented in Fig. 5, it is concluded that for all possible fault types and locations, the protection scheme will work properly according to the sequence of recloser-fuse operation depicted in Fig. 1a.

5.2 Allocation and Sizing of Distributed Energy Resource

The optimized allocation and sizing of DER in the IEEE 34-Node Test Feeder was carried out considering the recloser–fuse coordination constraints in order to preserve the protection scheme proposed in Sect. 5.1. Regarding the operational limits of the system, the voltage limits are, respectively, 0.88 and 1.10 pu (IEEE, 2018); the current limits were defined according to the line section configuration; and the minimum lagging and leading power factor is 0.8 (Rueda-Medina et al., 2013). With respect to the DER limits, the reactive power capability was based on the Standard IEEE 1547-2018 (IEEE, 2018), and it was assumed that three photovoltaic systems are available for allocation. The DER and substation energy costs are 0.03 and 0.15 US$/kWh, respectively (Rueda-Medina et al., 2013); and the DER capacities are 50 kW, with 10,000 US$ of annualized investment cost, and 100 kW, with 20,000 US$ of annualized investment cost (Rueda-Medina et al., 2013). Thus, considering the mathematical formulation of the DER allocation and sizing problem, it was possible to reach the Pareto set approximation, shown in Fig. 6. In the graphs of Fig. 6, the value of 100%, present in the short-circuit and voltage deviation axis, corresponds to the system without DERs.

Based on Fig. 6b, it is noticed that the objective functions f_4 (investment cost) and f_5 (voltage deviation) are non-conflicting objectives; consequently, it is possible to achieve the optimized solution considering only f_4 and f_5. Nevertheless, the objective functions f_6 (short-circuit current) and f_4, presented in Fig. 6c, are conflicting objectives; thus, the attenuation of the costs promotes an increase in the short-circuit current, due to the fault current contribution of the inverter-based DER. The same behavior can be observed from the analysis of the objective functions f_6 and f_5, which are shown in Fig. 6d. All the solutions, present in the Pareto set approximation, are equally valid from the point of view of multi-objective optimization. Therefore, the distribution system operator can choose any of these solutions depending on the decision maker's preferences.

In this paper, the solution which mutually minimizes f_4 and f_5, highlighted in red in Fig. 6a, was chosen, since the

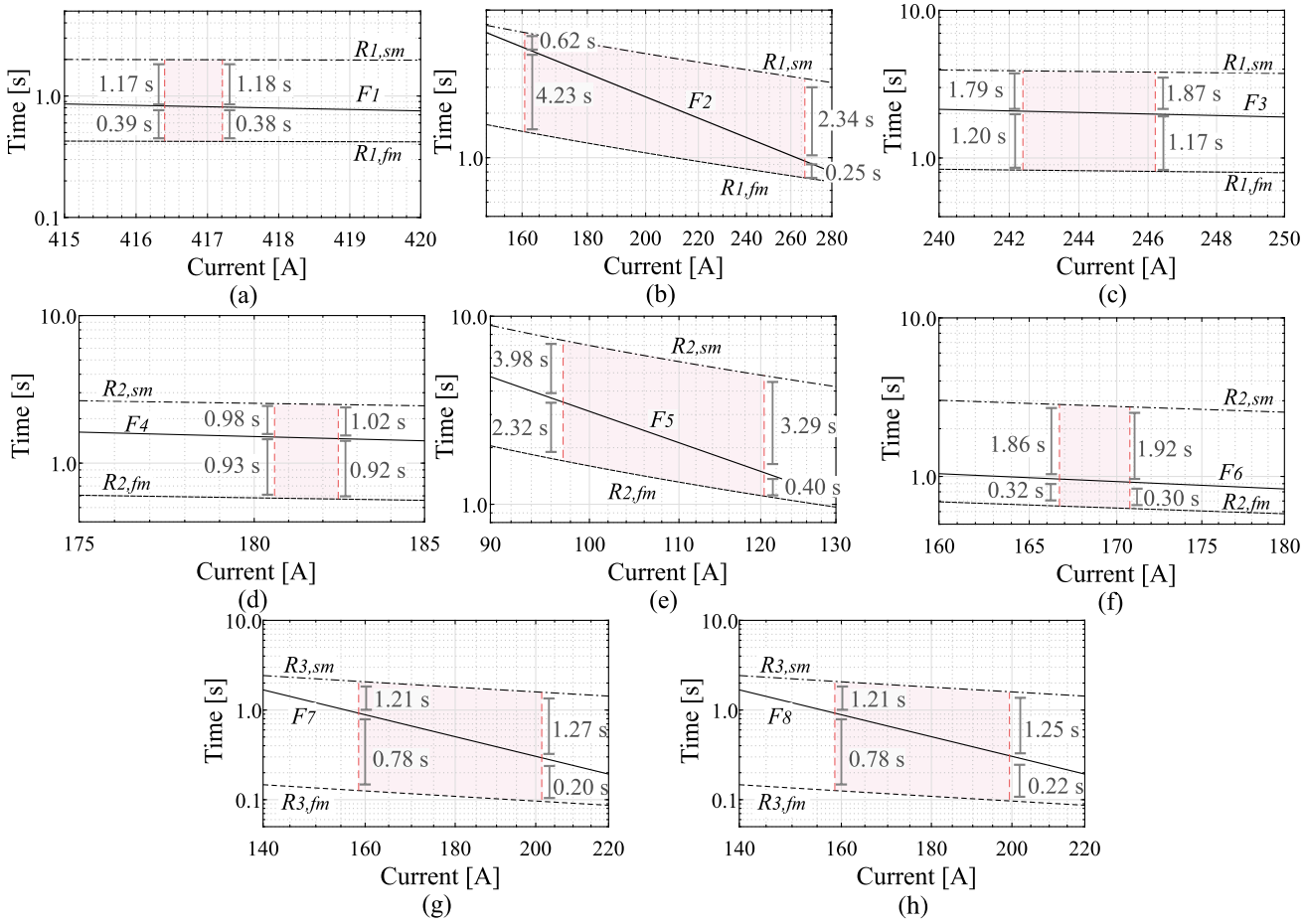

Fig. 5 Coordination between the reclosers and fuses: **a** F_1, **b** F_2, **c** F_3, **d** F_4, **e** F_5, **f** F_6, **g** F_7, and **h** F_8

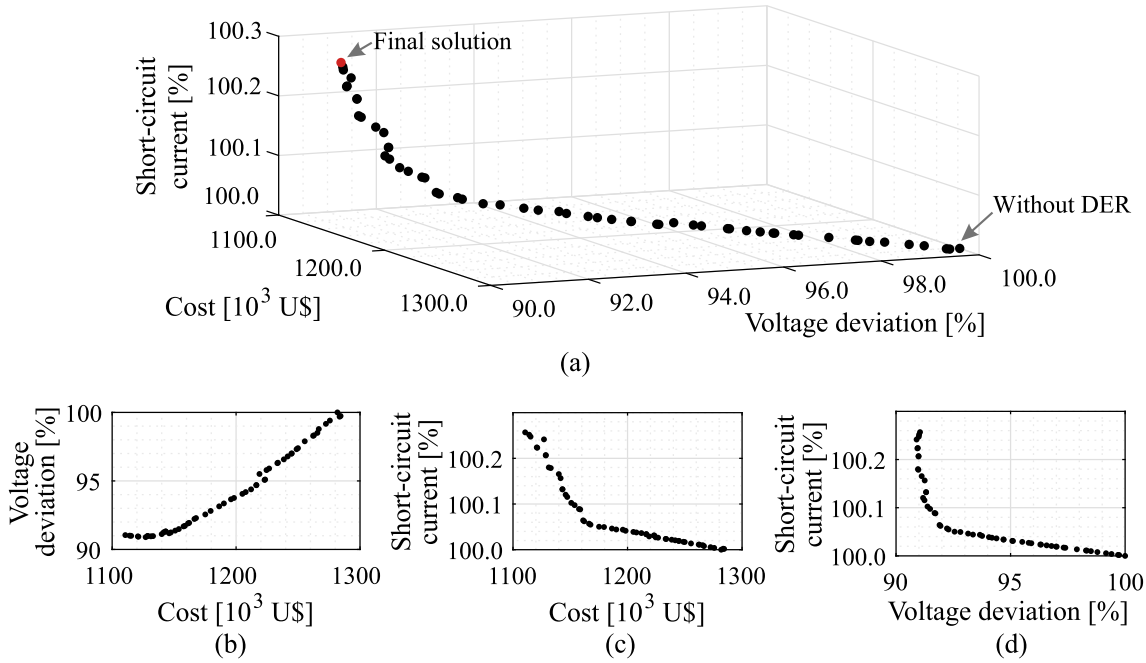

Fig. 6 Pareto set approximation for the problem of DER sizing and allocation: **a** three-dimensional chart, **b** vertical view, **c** left view, and **d** front view

fault current increased by only 0.26%. From this solution, it was possible to achieve a 15.61% and 10.01% reduction in the overall cost and voltage deviation, respectively, when compared to the system without DER. The slight short-circuit current variation, observed in the Pareto set approximation, is due to the DER locations selected by the NSGA-II combined with the voltage-dependent control modes adopted in this study, which limit the fault current contribution of the DER. The chosen solution presents DERs in nodes 19, 21 and 28, with active power of 100, 100 and 100 kW, and reactive power of 26, 22 and 12 kVAr, respectively. From the probabilistic scenarios generated by the MCS, it is possible to obtain the voltage in each node of the feeder considering the system without and with DERs. These statistical results are exposed in Fig. 7 using a boxplot. It is important to mention that the voltage and current data, shown in this paper, were measured between 8 and 16 h, since this time interval presents the highest generation levels.

By comparing Fig. 7a and b, it can be observed that the DER integration promoted an improvement in the voltage profile. In this context, the minimum and maximum values (disregarding the outliers) and the lower and upper quartile of the voltage values shifted up. In addition, the variation of the voltage magnitude median along the distribution system was reduced when considering the optimized solution. This reduction is due to the objective function f_2, which minimized by 10.01% the voltage deviation of the system.

The load current of the IEEE 34-Node Test Feeder is presented in Fig. 8, considering the system without and with DERs. From Fig. 8a and b, it can be noted that the system with DERs presents lower load current values compared to the system without DER. The study conducted by Mendes et al. (2021) provides supporting evidence for the observed reduction, demonstrating that the allocation of DERs contributes to the minimization of the distribution network currents. The research findings emphasize the significant influence of DERs location and size on the load current; consequently, the proper allocation and sizing of DERs in the system become crucial for optimizing the overall system performance, since the load current decrease leads to the minimization of the network power losses (Priya et al., 2022).

The fault current was exposed only for the scenario with the DERs allocated in the distribution system, since the short-circuit currents are not substantially modified by the DER integration, as depicted in Fig. 6. Figure 9 shows a boxplot

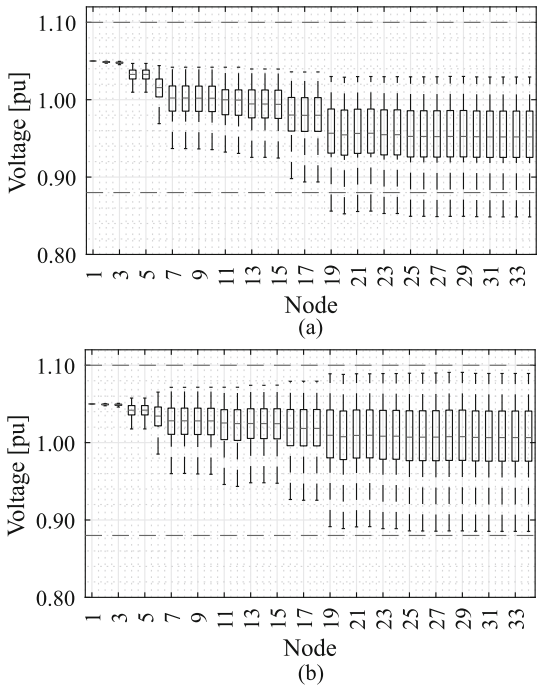

Fig. 7 Voltage profile considering the system: **a** without DER and **b** with DER

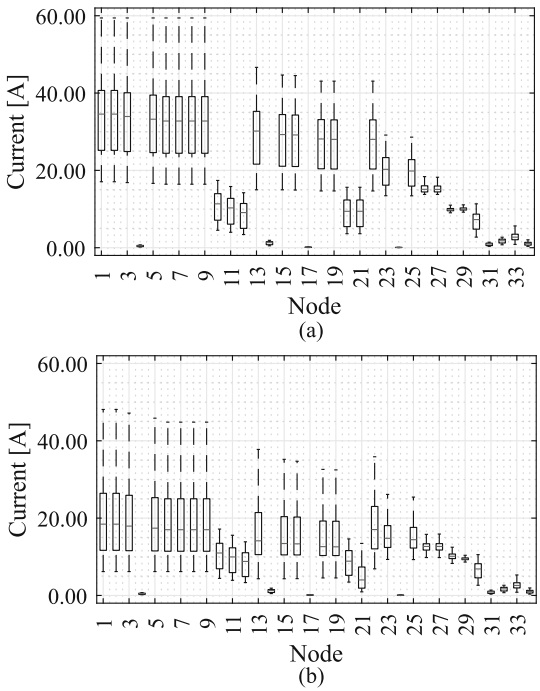

Fig. 8 Load current considering the system: **a** without DER and **b** with DER

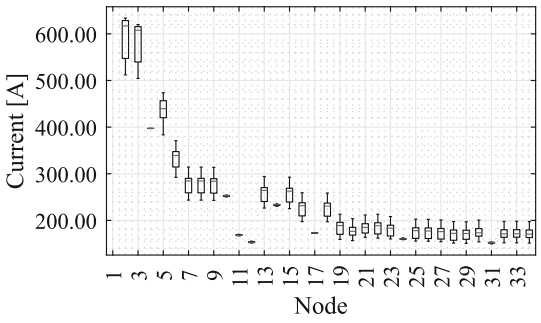

Fig. 9 Short-circuit current measured at the faulted node considering a fault application in each node of the system

of this current considering all fault types (three line, three line-to-ground, line-to-ground, line-to-line and line-to-line-to-ground) and the probabilistic scenarios generated by the MCS. It is important to highlight that the x-axis corresponds to the node in which the fault is applied. From Fig. 9, it is possible to observe the substantial variation of the short-circuit current considering all the fault types and the stochastic nature of the generation and load profile. Furthermore, the fault current reduces as far as the fault moves away from the substation, due to the increase in the line section impedance.

Taking Figs. 8 and 9 into account, it noticed the importance of considering all fault types and the generation and load uncertainties in both mathematical formulations (coordination of protective devices and DERs allocation), since these variables interfere directly in the adjustment of protective devices. Therefore, through the proposed methodology, it is possible to ensure the minimization of the objective functions present in Eqs. (1)–(3) and (16)–(18), and the correct coordination of reclosers and fuses, regardless of the fault type and location, for the system with and without DERs.

6 Conclusion

In this paper, a protection scheme composed of reclosers and fuses was proposed, considering the NSGA-II algorithm to mutually minimize the operating time of each protective device. Furthermore, this multi-objective optimization algorithm was also used to optimize the size and location of DERs in the IEEE 34-Node Test Feeder. The objectives of this allocation problem consist of the minimization of the investment and operation costs, the voltage deviation and the short-circuit current. The addition of the short-circuit current in the mathematical formulation assisted in the maintenance of the original protection scheme, since the fault current increased by only 0.26% when considering the DERs allocated in the distribution system.

Another important contribution of this work is the inclusion of the recloser–fuse coordination constraints in the formulation of the DER allocation and sizing problem, which preserved the correct operation of the protection scheme proposed in this study. Taking this novel approach into account, it is possible to avoid the need for adaptive protection schemes, the application of FCL and the adjustment of the protective device settings considering the DER integration in the system, which are the most adopted solutions in recent papers.

Regarding the DER allocation results, it observed a 15.61% reduction in the overall cost, due to the lower DER energy cost when compared to the substation energy cost. In addition, the voltage deviation of the system was reduced by 10.01%, caused by the minimization of the current of each branch, which decreases the power losses of the network.

The time-series-based probabilistic approach, carried out through the MCS, made it possible to consider the uncertainties of the loads and power generated by each DER, in addition to ensuring that the recloser–fuse coordination constraints and the system operational constraints are met for the 24 h of the day and for all the probabilistic scenarios generated by the MCS. Finally, considering the proposed methodology, it is possible to take advantage of the DER integration and mitigate the issues caused by this new scenario (mis-coordination between protective devices), without adding investment and operational cost.

In future works, it is important to consider the inclusion of other types of DERs since they present distinct behaviors under fault conditions, which can significantly impact the proper operation of protective devices. Each DER technology may introduce unique challenges and considerations regarding fault response and protective devices' coordination.

Acknowledgements This study was financed by the Fundação de Amparo à Pesquisa e Inovação do Espírito Santo— Brazil (FAPES)— Number 026/2021.

Declarations

Conflicts of interest All authors declare that they have no conflict of interest.

References

Abdelaziz, M., & Moradzadeh, M. (2019). Monte-Carlo simulation based multi-objective optimum allocation of renewable distributed generation using OpenCL. *Electric Power Systems Research, 170*, 81–91. https://doi.org/10.1016/j.epsr.2019.01.012

Ahmadi, B., Ceylan, O., & Ozdemir, A. (2021). Distributed energy resource allocation using multi-objective grasshopper optimization algorithm. *Electric Power Systems Research, 201*(107), 564. https://doi.org/10.1016/j.epsr.2021.107564

Alam, M. N. (2019). Adaptive protection coordination scheme using numerical directional overcurrent relays. *IEEE Transactions on Industrial Informatics, 15*, 64–73. https://doi.org/10.1109/TII.2018.2834474

Alam, M. N., Das, B., & Pant, V. (2018). Optimum recloser-fuse coordination for radial distribution systems in the presence of multiple distributed generations. *IET Generation, Transmission & Distribution, 12*, 2585–2594. https://doi.org/10.1049/iet-gtd.2017.1532

Blaabjerg, F., Yang, Y., Yang, D., et al. (2017). Distributed power-generation systems and protection. *Proceedings of the IEEE, 105*, 1311–1331. https://doi.org/10.1109/JPROC.2017.2696878

Cheng, C. S., & Shirmohammadi, D. (1995). A three-phase power flow method for real-time distribution system analysis. *IEEE Transactions on Power Systems, 10*(2), 671–679. https://doi.org/10.1109/59.387902

Dahej, A. E., Esmaeili, S., & Hojabri, H. (2018). Co-optimization of protection coordination and power quality in microgrids using unidirectional fault current limiters. *IEEE Transactions on Smart Grid, 9*, 5080–5091. https://doi.org/10.1109/TSG.2017.2679281

Deb, K., Pratap, A., Agarwal, S., et al. (2002). A fast and elitist multiobjective genetic algorithm: NSGA-II. *IEEE Transactions on Evolutionary Computation, 6*(2), 182–197. https://doi.org/10.1109/4235.996017

Dehghanpour, E., Kazemi Karegar, H., Kheirollahi, R., et al. (2018). Optimal coordination of directional overcurrent relays in microgrids by using cuckoo-linear optimization algorithm and fault current limiter. *IEEE Transactions on Smart Grid, 9*, 1365–1375. https://doi.org/10.1109/TSG.2016.2587725

Eaton (2018) Electrical and industrial: Power management solutions. https://www.eaton.com/. Accessed 9 July 2023.

El-Ela, A. A. A., El-Sehiemy, R. A., Shaheen, A. M., et al. (2021). Optimal allocation of distributed generation units correlated with fault current limiter sites in distribution systems. *IEEE Systems Journal, 15*, 2148–2155. https://doi.org/10.1109/JSYST.2020.3009028

Elmitwally, A., Gouda, E., & Eladawy, S. (2016). Restoring recloser-fuse coordination by optimal fault current limiters planning in DG-integrated distribution systems. *International Journal of Electrical Power & Energy Systems, 77*, 9–18. https://doi.org/10.1016/j.ijepes.2015.11.021

Fani, B., Bisheh, H., & Karami-Horestani, A. (2018). An offline penetration-free protection scheme for PV-dominated distribution systems. *Electric Power Systems Research, 157*, 1–9. https://doi.org/10.1016/j.epsr.2017.11.020

Ferraz, R. S. F., Ferraz, R. S. F., Rueda-Medina, A. C., et al. (2020). Genetic optimisation-based distributed energy resource allocation and recloser-fuse coordination. *IET Generation, Transmission & Distribution, 14*, 4501–4508. https://doi.org/10.1049/iet-gtd.2020.0664

Hamidi, M. E., & Chabanloo, R. M. (2019). Optimal allocation of distributed generation with optimal sizing of fault current limiter to reduce the impact on distribution networks using NSGA-II. *IEEE Systems Journal, 13*, 1714–1724. https://doi.org/10.1109/JSYST.2018.2867910

Huang, D., Li, H., Cai, G., et al. (2019). An efficient probabilistic approach based on area grey incidence decision making for optimal distributed generation planning. *IEEE Access, 7*, 93175–93186. https://doi.org/10.1109/ACCESS.2019.2927713

IEC. (1989). Electrical relays—part 3: Single input energizing quantity measuring relays with dependent or independent time. International Electrotechnical Commission (IEC).

IEEE. (2018). IEEE standard for interconnection and interoperability of distributed energy resources with associated electric power systems interfaces. IEEE Std 1547–2018 (Revision of IEEE Std 1547-2003) pp 1–138. https://doi.org/10.1109/IEEESTD.2018.8332112

Jain, R., Lubkeman, D. L., & Lukic, S. M. (2019). Dynamic adaptive protection for distribution systems in grid-connected and islanded modes. *IEEE Transactions on Power Delivery, 34*, 281–289. https://doi.org/10.1109/TPWRD.2018.2884705

Kersting, W.H. (2001) Radial distribution test feeders. In: Conference Proceedings 2001 IEEE Power Engineering Society Winter Meeting. vol. 2, pp 908–912, https://doi.org/10.1109/PESW.2001.916993.

Mathur, A., Pant, V., & Das, B. (2015). Unsymmetrical short-circuit analysis for distribution system considering loads. *International Journal of Electrical Power & Energy Systems, 70*, 27–38. https://doi.org/10.1016/j.ijepes.2015.02.003

Mathur, A., Das, B., & Pant, V. (2017). Fault analysis of unbalanced radial and meshed distribution system with inverter based distributed generation (IBDG). *International Journal of Electrical Power & Energy Systems, 85*, 164–177. https://doi.org/10.1016/j.ijepes.2016.09.003

Mendes, M. A., Vargas, M. C., Simonetti, D. S. L., et al. (2021). Load currents behavior in distribution feeders dominated by photovoltaic distributed generation. *Electric Power Systems Research, 201*(107), 532. https://doi.org/10.1016/j.epsr.2021.107532

Meskin, M., Domijan, A., & Grinberg, I. (2020). Impact of distributed generation on the protection systems of distribution networks: Analysis and remedies—review paper. *IET Generation, Transmission & Distribution, 14*, 5944–5960. https://doi.org/10.1049/iet-gtd.2019.1652

Pereira, K., Pereira, B. R., Contreras, J., et al. (2018). A multiobjective optimization technique to develop protection systems of distribution networks with distributed generation. *IEEE Transactions on Power Systems, 33*, 7064–7075. https://doi.org/10.1109/TPWRS.2018.2842648

Priya, P. P. R., Baskar, S., Selvi, S. T., et al. (2022). Optimal allocation of distributed generation using evolutionary multi-objective optimization. *Journal of Electrical Engineering & Technology*. https://doi.org/10.1007/s42835-022-01269-y

Purwar, E., Singh, S. P., & Vishwakarma, D. N. (2020). A robust protection scheme based on hybrid pick-up and optimal hierarchy selection of relays in the variable DGs-distribution system. *IEEE Transactions on Power Delivery, 35*, 150–159. https://doi.org/10.1109/TPWRD.2019.2929755

Roy, N. B., & Das, D. (2021). Optimal allocation of active and reactive power of dispatchable distributed generators in a droop controlled islanded microgrid considering renewable generation and load demand uncertainties. *Sustainable Energy, Grids and Networks, 27*(100), 482. https://doi.org/10.1016/j.segan.2021.100482

Rueda-Medina, A. C., Franco, J. F., Rider, M. J., et al. (2013). A mixed-integer linear programming approach for optimal type, size and allocation of distributed generation in radial distribution systems. *Electric Power Systems Research, 97*, 133–143. https://doi.org/10.1016/j.epsr.2012.12.009

Shah, P. H., & Bhalja, B. R. (2014). New adaptive digital relaying scheme to tackle recloser-fuse miscoordination during distributed generation interconnections. *IET Generation, Transmission & Distribution, 8*, 682–688. https://doi.org/10.1049/iet-gtd.2013.0222

Sharma, A., & Panigrahi, B. K. (2018). Phase fault protection scheme for reliable operation of microgrids. *IEEE Transactions on Industry Applications, 54*, 2646–2655. https://doi.org/10.1109/TIA.2017.2787691

Shih, M. Y., Conde, A., Leonowicz, Z., et al. (2017). An adaptive overcurrent coordination scheme to improve relay sensitivity and overcome drawbacks due to distributed generation in smart grids. *IEEE Transactions on Industry Applications, 53*, 5217–5228. https://doi.org/10.1109/TIA.2017.2717880

Shu, Z., Chen, Y., Deng, C., et al. (2021). Pareto optimal allocation of flexible fault current limiter based on multi-objective improved bat algorithm. *IEEE Access, 9*, 12762–12778. https://doi.org/10.1109/ACCESS.2021.3050795

Usama, M., Mokhlis, H., Moghavvemi, M., et al. (2021). A comprehensive review on protection strategies to mitigate the impact of renewable energy sources on interconnected distribution networks. *IEEE Access, 9*, 35740–35765. https://doi.org/10.1109/ACCESS.2021.3061919